3-7 Measurement of Brain Activity by Near Infrared Light

EDA Hideo

Non invasive brain measurement systems are widely used for the brain research. There are two kind of equipment. Ones measure electro-magnetic signal from the brain by EEG or MEG. Others measure hemodynamic response by fMRI or NIRS. Development of analysis and research tool is also important for the brain research. NIRS calculates changes in hemoglobin parameters. We compared images by fMRI with images by NIRS. These agreed quite well.

Keywords
Brain activity, Non-invasive measurement, Hemodynamic response, Near infrared light, Spectroscopy,

1 Introduction

There are various approaches to brain research. Among these, measurement of human brain activity and analysis of resultant images has developed rapidly in the last decade. Brain-activity measurement instruments used in these cases are also used in medical practice, and were not originally designed by researchers. Researchers must thus ensure that these systems have passed rigorous manufacturer examinations if these systems are to be used in research.

Determining methods of measuring the brain and the types of conclusions that are to be drawn from measured values represent significant tasks. Before drawing such conclusions, it may first be necessary to examine seriously whether the obtained data can support detailed analysis. Our group established as one of its research tasks the development of specific tools for brain research, as detailed analysis of brain research cannot be carried out if we simply accept the current tools, and consequently we must devise tools specifically tailored to the tasks at hand.

In the main part of this paper, we will first present an overview of the objects of non-invasive brain-activity measurement with the instruments currently in use. We will then provide a description of the principles and applications of brain-activity measurement using light.

2 Visualization of tissue

Physical phenomena involving ultrasonic phenomena, electromagnetic waves, X-rays, light, and so on all involve waves. Through the use of these waves, a living body can be measured and visualized. Technology to visualize the interior of the living body has long been sought after in the field of medicine, with X-ray tomography (X-ray CT) and magnetic resonance imaging (MRI) now indispensable in medical practice. Measuring tissue without incision is referred to as “non-invasive” in English, and the JIS has stipulated use of the Japanese term “mu-shinshu” (non-invasive) to denote this medical practice. (Currently, the term “hi-shinshu (also “non-invasive”) is often used in Japanese.)

X-ray CT began with a paper by Hounsfield published in the British Journal of Radiology in 1973. Subsequently, an X-ray CT image of the head was presented by Ambrose et al. For MRI, Lauterbur published a paper in Nature in 1973, the same year as the initial report on X-ray CT. In 1978, the company EMI presented a number of MRI images of the brain. Both X-ray CT and MRI have brought Nobel prizes to the researchers involved.

It is very interesting that in each case of these initial reports the brain was the measurement target. In terms of obtaining a structural image, the brain is not a particularly difficult organ to image relative to other internal organs. Organs involving intense movement, such as the heart, are far more difficult to view (in fact the technological challenges of heart imaging have formed a core target of significant past research). In terms of radiology, the origin of human body imaging even today remains the heart. Accordingly, images of the brain are from below (roughly from the position of the heart), and, consequently, the resultant brain image must be mirror-reversed to correspond to the actual position of the brain relative to the exterior of the subject. If the brain is displayed as viewed from above, not from below, the right/left orientation of the image coincides with that of the actual structure, rendering the brain image easier to understand. However, we must note that images taken from above are different from conventional images, with the heart located in the origin.

Any device that measures human characteristics through interior imaging irradiates waves to the living body and produces image information based on the degree to which these waves are absorbed based on signal reflections from the body. The waves may be classified as sonic waves or electromagnetic waves, depending on wavelength. One characteristic of the waves used in somatometry is minimal absorption by water. Since it can safely be said that most of the living body consists of water, this characteristic can be phrased conversely: waves at wavelengths at which absorption by water is minimal are used in somatometry because such waves can easily penetrate the living body. On the other hand, devices exist to measure the waves emitted spontaneously by the living body, including equipment used in electroencephalography (EEG) and magnetoencephalography (MEG). These devices operate at wavelengths resistant to absorption by water. Additionally, positron emission tomography (PET) provides important metabolic data through the injection of a radioisotope and subsequent detection of the gamma rays issued from the interior of the body.

The diagnostic imaging equipment described above can be divided roughly into devices that display structural images of the living body and those that display functional images. Images used in brain research are appropriately referred to as functional images, which differ significantly from structural images in a number of respects. The presentation of functional MRI (fMRI) by Ogawa in 1992 [1] is now viewed as a monumental achievement in the imaging/measurement of brain activity. Figure 1 shows an explanatory diagram of Blood oxygenation level dependent (BOLD) signal. Ogawa et al. gave a purely physical explanation (the right-hand part of Fig. 1), while the other explanation (the left-hand part of the Fig. 1) was added separately.

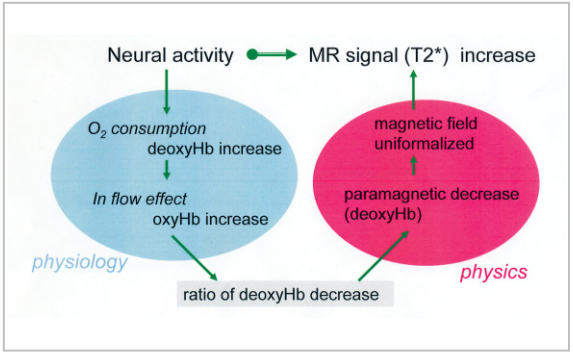

Fig. 1 *Explanation of Blood Oxygenation Level Dependent signal*

This fMRI technology plays an enormous role in current brain research. However, it must be notes that an fMRI image is usually

comprised of statistical values. In other words, it does not show a general state of cerebral activity, but instead indicates the specific response of a given area to a stimulus. A threshold response is set to enable statistical calculation of the correspondence between stimulus and the area in question. The selection of this threshold value is very important: if the threshold is too low, the image may indicate that every site is active. The type of stimulus also affects the results, as with the selection of the threshold. Therefore, in brain imaging, it is extremely important to generate a precise stimulus that activates only the target area.

3 What should be measured in brain research? At what resolution?

If brain activity is considered from a microscopic viewpoint, a neuron fires, a metabolic motion is initiated, and there is a hemodynamic response change. Figure 2 shows a diagram illustrating the principles of fMRI. Firing of the neurons results in activity between various areas in the brain, finally resulting in consciousness and qualia—a range of higher brain functions. When studying these higher brain functions, it may be said that the issues involved may only be addressed after images of all neurons and their hemodynamic responses are obtained with high temporal resolution. However, since measurement of the head and analysis of the resultant images remains a topic of discussion, brain research must proceed based on incomplete images with bold conjecture. Further, even if the activity of all neurons could be measured, we would quickly lose our way among the innumerable resultant graphs, estimated to number roughly twelve billion.

The primary object of brain measurement is considered to be the state of neural activity. Simply speaking, measurement of such neural activity would have to be on the order of millimeters in terms of spatial resolution and on the order of milliseconds in terms of time. Further, when measuring the hemodynamic

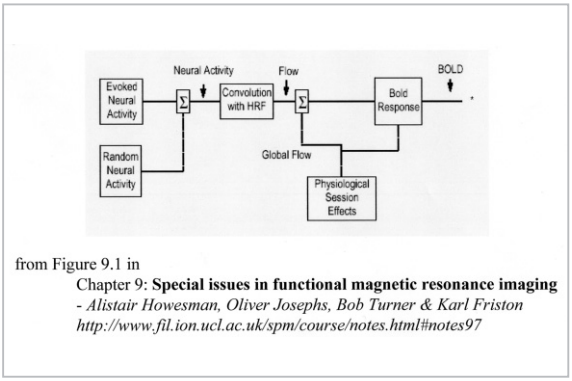

from Figure 9.1 in
Chapter 9: **Special issues in functional magnetic resonance imaging**
- Alistair Howesman, Oliver Josephs, Bob Turner & Karl Friston
http://www.fil.ion.ucl.ac.uk/spm/course/notes.html#notes97

Fig.2 *From Neural activity to BOLD*

response following neural activity target spatial resolution is on the order of less than a centimeter, at a temporal resolution of less than a second. However, as shown in Fig. 2, the brain is active even without external stimuli. In this context we must emphasize once again the fundamental importance of distinguishing spontaneous activity from activity evoked by a stimulus.

4 Theory of measurement of light absorption

Equipment for non-invasive measurement of brain activity using light can be divided into two categories: devices that translate values calculated by the modified Lambert-Beer's law into images; and devices that convert absorption coefficients into images through an inverse calculation of a light-diffusion equation. Included among the former category are optical topography and near-infrared spectroscopic (NIRS) imaging systems, while the latter category consists primarily of optical CT (computed tomography) or diffused tomography. Devices of the former type currently play an active role in brain research. However, reliable results will not be obtained unless the special features of these devices are adequately understood. Here we will introduce a brief history of the theory involved, beginning with Lambert-Beer's law (which has come to form the underlying basis of hemoglobin-related calculations) and leading up to the modified Lambert-Beer's law currently in use.

4.1 History of Lambert-Beer's law

Lambert-Beer's law forms the basis of measurement by light. This indicates, as shown in Fig. 3, that absorbance, expressed logarithmically as an intensity ratio of incident light to detected light, is proportional to the product of the distance between the site of incidence and the site of detection and the concentration of the target material. This law is occasionally simply referred to as Beer's law. However, if one were to list the names of the researchers contributing to this law in order, it would properly be referred to as Bouguer-Lambert-Beer's law. We describe this law throughout as Lambert-Beer's law.

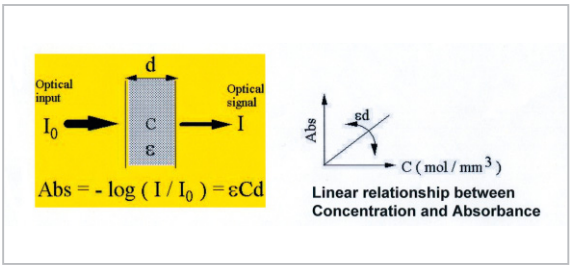

Fig.3 *Lambert-Beer's law*

A brief history of this law begins with reference to the writings of S. F. Johnston [2] and other writings. In the 18th to 19th centuries, when this law was formulated, science was not as specialized as it is today. The most well-known figures in this era produced achievements in various fields. Thus it is interesting to note that none of these figures may be referred to as a researcher in a specific field.

Pierre Bouguer, a French physicist and geodesist (1698–1758) published his "Essai d'optique sur la generation de la lumière" on the radiation of light in 1729. Bouguer assumed that light radiation obeys a particular law (the inverse-square law) stipulating that the radiation of light is in inverse proportion to the square of the distance traveled. He developed original observation equipment, established a method of determining brightness with the naked eye, illustrating the concept with a comparison of brightness between the moon and a candle. Further, Bouguer reported in his essay that a change in brightness shows exponential dependence on the distance from the light source, based on the results of these observation experiments.

Johann Heinrich Lambert (1728–1777), born in France, was a philosopher, a physicist, a mathematician, and an astronomer; he published his "Photometria" in 1760, presenting a formulation of the phenomenon in which the intensity of light decreases as an exponential function of distance from the light source, as follows:

$$I = I_0 \exp(-k\,d)$$

In this formula, I denotes observed light intensity, I_0 irradiated light intensity, d the distance from the light source, and k a proportional constant.

In brief, the phenomenon in which the intensity ratio of detected light decreases exponentially with an increase in distance between detected and incident light was first observed by Bouguer and later formulated by Lambert.

August Beer (1825–1863), a German mathematician, chemist, and physicist, published a paper in 1852 in which he discussed the phenomenon in which light decreases exponentially according to the concentration of the target material. He published his work on optics entitled "Einleitung in die höhere Optik" in 1854.

As described above, Lambert-Beer's law, the foundation of all current spectroscopy theory, was established through the achievements of Bouguer, Lambert, and Beer.

The formula is expressed as follows:

$$\text{Absorbance} = -\log(I/I_0) = k\,C\,d,$$

where C denotes the concentration of the material. Since absorbance itself is a non-dimensional figure, the proportionality coefficient k of this formula features the following dimension: {inverse of (product of distance d

and concentration C)}; this is referred to as the molecular extinction coefficient. The principle of analysis applied by the spectrophotometer entails the measurement of I/I_0 and computation of concentration C through prior determination of the coefficient k and the optical path length of distance d.

4.2 Practice of spectroscopic analysis

The fundamental structure of the spectroscopic analyzer includes a light source, a monochromatizing device, a detector, and a cell in which the sample is housed, among other components. Although Lambert-Beer's law is a simple and convenient method of quantitatively measuring concentration, certain limitations to the application of this law have been indicated. For example, the law assumes a sample target featuring a low density concentration; also, if the sample is localized, flattening occurs; additionally, the law applies only to one-dimensional quantitative measurement of a sample containing only absorbing materials.

If the concentration is dense, the problem of molecular interaction arises, and consequently the relation between absorbance and concentration deviates from a straight line. As shown in Fig. 4, when the material is non-uniform i.e., when it is "localized," a phenomenon referred to as "flattening" may occur. This can easily be understood by thinking of the relationship between hemolyzed hemoglobin and red blood cells. If red blood cells are hemolyzed, hemoglobin is distributed uniformly and absorption measurement becomes possible. In contrast, if hemoglobin exists only in red blood cells, the measured concentration often appears very low, even when the actual concentration is the same as in the case of even, uniform distribution. This is because, in the case of non-hemolyzed red blood cells, light passes through the red blood cells with no absorption; thus the peak of the absorption spectrum appears smaller (i.e., flattened). The term "flattening" is derived from this phenomenon. Finally, if a tissue contains non-absorbing substances, light may be diverted from the detector by scattering. Since determination as to whether attenuation observed by the detector is caused by absorption or by scattering is impossible, the presence of scattering may represent a source of error.

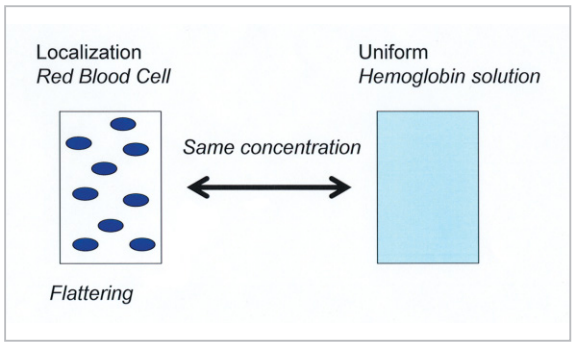

Fig.4 *Flattering by localization*

Each device has its own dynamic range of measurement, and these devices often feature a sample holder approximately 1 cm length. Based on this hardware-specific restriction, light transmitted through a particularly thick sample may be too weak to measure. In this case, the sample is diluted until it is measurable. Furthermore, two samples, a reference and a sample, are normally prepared. The measured amount of light for the reference is expressed by I_0 and the measured amount of light for the sample is expressed by I. Concentration is then calculated based on the difference between I_0 and I. In other words, an appropriate reference is chosen depending on the object of measurement. However, this procedure is not applicable in non-invasive human measurement. This is because when measuring human hemoglobin, the use of a sample holder is not applicable and living tissue cannot be diluted. Moreover, it is difficult to prepare a living reference sample in which the amount of hemoglobin is zero.

4.3 Treatment of light scattering

In spectroscopic analysis, the effects of phenomena other than absorption are roughly expressed as scattering. As shown in Fig. 5, scattering consists of light traveling in directions other than a straight line between the light source and the detector. However, to be

more accurate, if we imagine light colliding with particles in the sample one after another, collisions that decrease energy are collectively referred to as absorption and collisions that do not affect energy levels are collectively referred to as scattering.

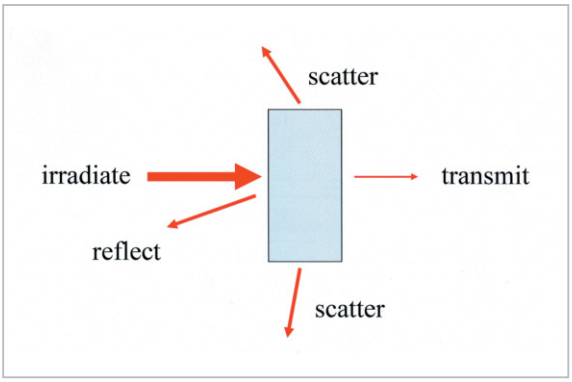

Fig.5 *Scattering*

Particles below a certain size in an absorbing material will cause light to be scattered. Theoretical analyses assuming such non-homogeneity had been proposed from the 1960s through the 1970s, and a number of related reports are available. One avenue of research involved measurement of hemoglobin concentration without hemolyzation [3]. Extension of studies from single scattering caused by a single particle to multiple scattering caused by multiple particles is also being considered [4].

Optical scattering includes both scattering that changes the wavelength and scattering that does not change the wavelength. In somatometry, Rayleigh scattering and Mie scattering [5], which do not change the wavelength, must be taken into consideration. If scattering is handled as an interaction between a photon and particles, it is first necessary to determine the wavelength and the size of the relevant particles. If the scattering particles are smaller than the wavelength of light, the Rayleigh scattering formula is used. (The relationship between particle size and wavelength is often used to explain why the sky is blue and why sunsets are red.) Moreover, when the scattering particles are of approximately the same size as the wavelength of light, the Mie scattering formula (which is more complex than the Rayleigh scattering formula) is instead applied in analysis. Assuming a measurement wavelength of 800 nm, the size of a single cell will be equivalent to or smaller than the wavelength, whereas the red blood cell is on the order of a few microns and hence is comparable to the wavelength in size. However, the living body is inhomogenous at all levels, from red blood cells to vessels to tissues and internal organs. It is in any case awkward to apply a single scattering theory based on a given physical treatment and to perform analysis accordingly; scattering therefore must be treated in a macroscopic manner. One procedure to treat scattering macroscopically involves an optical diffusion equation and the modified Lambert-Beer's law.

4.4 From a transport equation to an optical diffusion equation

Generally, irradiating light to the living body and generating an image based on absorption is referred to as quantitative measurement within a "turbid" system. An example of a turbid system can be seen in the use of automobile headlights to view the road in a dense fog. Monitoring the ground from a satellite through cloud cover is a similar example.

When analyzing how light is transmitted while being absorbed and scattered on a macroscopic level, the transport equation [6] [7], or the radiation equation [8] can be applied. The transport equation has been used to describe the movement of electrons and holes in a semiconductor and to illustrate the movement of thermal neutrons in a nuclear reactor. The radiation equation has been used for analysis of optical multiple scattering in the atmosphere. If both equations are moderately approximated in simplified forms, one can obtain an optical diffusion equation with three parameters: an absorption coefficient (1/mm), a scattering coefficient (1/mm), and an angular distribution of scattering. We have adopted this optical diffusion equation as the governing equation. Figure 6 summarizes a method

of deriving the diffusion equation from the transport equation according to an approach proposed by Kaltenbach et al. [9]. By diffusion approximation, the two parameters of the scattering coefficient and the angular distribution of scattering are now approximated by isotropic scattering, with the product of the two applied as a reduced scattering coefficient. Conventionally the diffusion constant D has been expressed using the formulas for the absorption coefficient and for the reduced-scattering coefficient, but this is in fact unreasonable, as this assumes that energy is lost due to absorption in the course of diffusion. Furutsu and Yamada focused attention on this problem and proposed a strict solution for the definition of D [10]. Subsequently, a formula containing only the reduced scattering coefficient has come to be used. As a result, research on the diffusion equation progressed significantly in the course of research into optical CT in the late 1980's and through the 1990's. However, imaging equipment based on the diffusion equation has yet to enter common use in the experimental field, largely because the calculations involved are extremely time-consuming.

4.5 Modified Lambert-Beer's law

Lambert-Beer's law is simple and convenient, and consequently its use in non-invasive human measurement has been subject to extensive investigation; the law is in fact currently under application in optical measurement [11]. This investigation has given rise to what is referred to as the modified Lambert-Beer's law, whose characteristics have given us the disadvantages of current topographic optical brain functional imaging. Therefore, an understanding of the modified law is essential.

When one intends to measure the living body, including scattering elements, using the sites of reflection and the like, Lambert-Beer's law can no longer be applied simply. The following equation is applied in a formulation similar to Lambert-Beer's law.

$$\Delta A = -\log(\Delta I / I_0) = \varepsilon \Delta C \langle d \rangle + \Delta S$$

For a structure such as that shown in Fig. 7, a linear relation is assumed between the change in concentration and the change in absorbance over a very short interval; the effect of the change in scattering is then

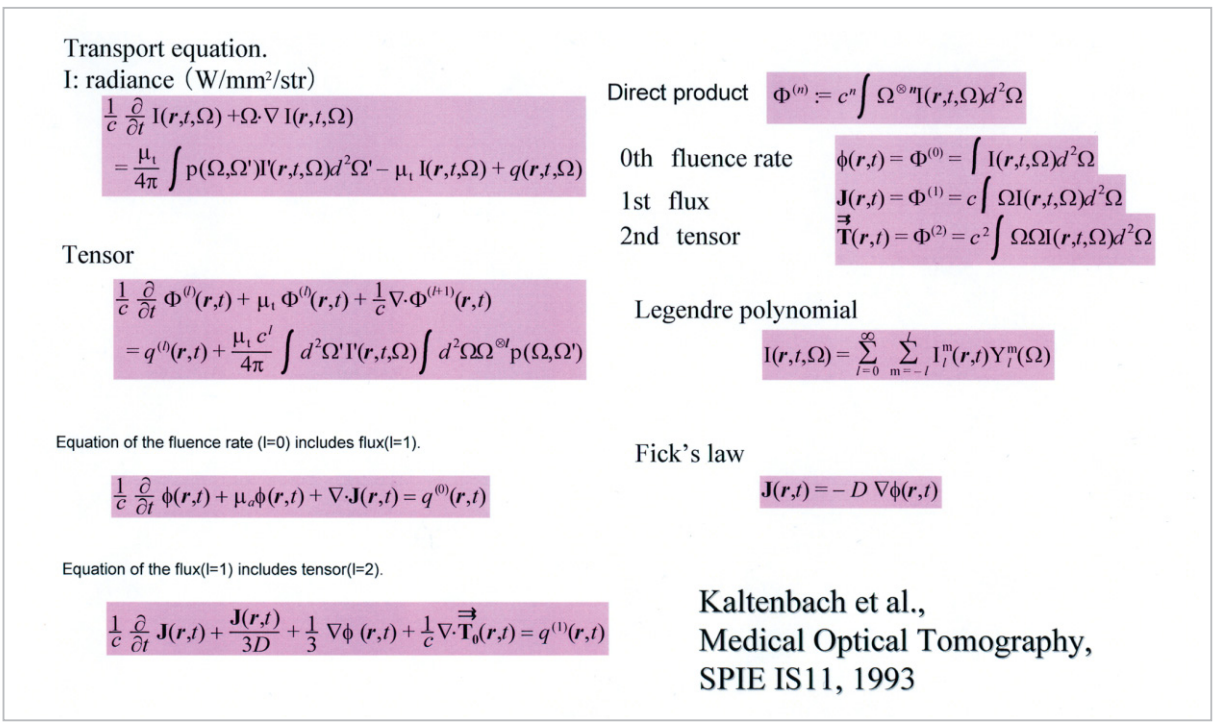

Fig.6 *Diffusion equation from the transport equation*

added. In order to calculate the concentration from measured values, it is sufficient to determine the three parameters appearing in this formula. Here, denotes the molecular extinction coefficient, C the change in concentration, <d> the mean optical path length, and S the scattering change. The appropriate method of determining these coefficients has long been the subject of investigation. For a case in which the concentration of hemoglobin is measured, three methods are available for each of the three parameters.

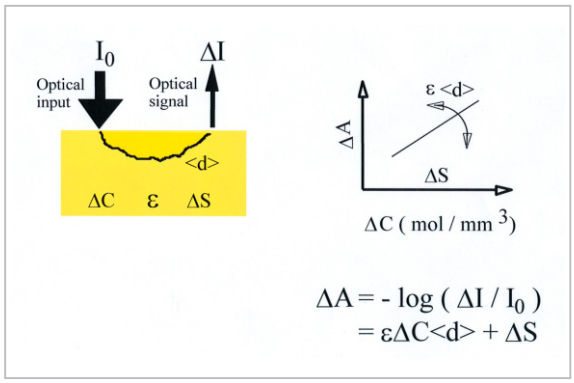

Fig.7 *Modified Lambert-Beer's law*

1 Molecular extinction coefficient

(1) Using the spectrum of pure hemoglobin; i.e., a reference spectrum or an experimentally obtained spectrum for hemolyzed blood
(Note that since there are two spectra for hemoglobin—one for the hemoglobin molecule and the other for the heme protein—care must be taken to select the appropriate spectrum.)
(2) Using a spectrum measured in vitro for hemoglobin into which a scatterer, such as milk, is mixed
(3) Using a spectrum measured in vivo for a rat head or other animal subject

2 Mean optical path length

(1) Setting to unity by ignoring the actual optical length
(2) Determining the coefficient for the optical path and multiplying the irradiation-to-detection distance by the coefficient
(3) Actual measurement of optical path length for each wavelength involved in measurement

3 Scattering change

(1) Setting to zero by ignoring the actual scattering change
(2) Setting to a constant featuring no dependence on the wavelengths used in measurement
(3) Setting to a different value for each measurement wavelength.

With respect to the molecular extinction coefficient 1 (1), Figure 8 shows the spectra for two types of hemoglobin. The left-hand vertical axis represents the spectrum of a hemoglobin molecule obtained by Matcher [12], and the right-hand vertical axis represents the spectrum of a heme protein by Zijlstra [13]. The hemoglobin molecule features four heme proteins. The four-fold quantitative difference between the right-and left-hand side vertical axes reflects the differences between the hemoglobin molecule and heme protein. When the change in hemoglobin is calculated using this spectrum, the same measured values result in an apparently four-fold difference, and care must be exercised to take this difference into account. In the hemoglobin calculation, the inverse matrix of the spectrum is used in multiplication, and consequently the hemoglobin calculated using the spectrum of the hemoglobin molecule becomes 1/4 times the value calculated using the spectrum of the heme protein.

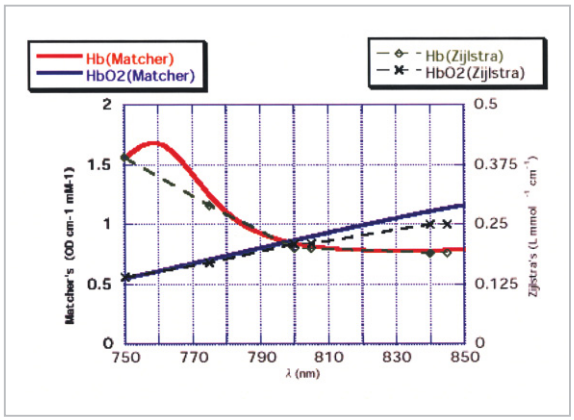

Fig.8 *Hemoglobin spectra*

As is the case with ordinary calculations

using Lambert-Beer's law, when the material to be measured consists of two substances, absorbance is calculated as the sum of the concentrations of the materials. Therefore, in a system in which the two components of oxygenated hemoglobin (oxyHb) and deoxygenated hemoglobin (deoxyHb) coexist, all that is required to calculate absorbance values for the two is to perform measurement using two or more wavelengths. Figure 9 shows a method of calculating hemoglobin based on absorbance when the molecular extinction coefficient is that of the hemoglobin molecule (method **1** (1) above corresponding to this parameter), the mean optical path length is unity (method **2** (1) for this parameter), and the scattering change is zero (method **3** (1) for this parameter). Since measured values at three wavelengths are obtained for two unknown parameters—oxyHb and deoxyHb—the concentration changes are calculated after determining a generalized inverse matrix. This procedure is equivalent to calculation using the least-squares method.

4.6 Problems with the modified Lambert-Beer's law

Generally, since linear approximation works only for very small sections, when the section becomes large error will increase. That is, when the change in concentration grows large in the modified Lambert-Beer's law, the measured value may not fully reflect this change. For reference, Fig. 10 shows a solution of the optical diffusion equation in an infinite medium. Actual optical propagation is more accurately shown by the solution of this diffusion equation for an actual medium. As can be seen in the graph, it is understood that the modified Lambert-Beer's law, which assumes a linear relation between concentration change and absorbance change, postulates a tangent to the actual curve. The gradient of this tangent is equivalent to the product of the molecular extinction coefficient and the mean optical path length. In our approach, in which the mean optical path is ignored, the value for hemoglobin is not calculated in units of concentration, but instead in a strange compound unit: the product of concentration and distance.

It is also significant that the gradient of the tangent varies depending on the position of contact. When calculating absorbance change, it is often the case that the original point of absorbance is set to a value corresponding to the time at the start of measurement. This original point of absorbance corresponds to

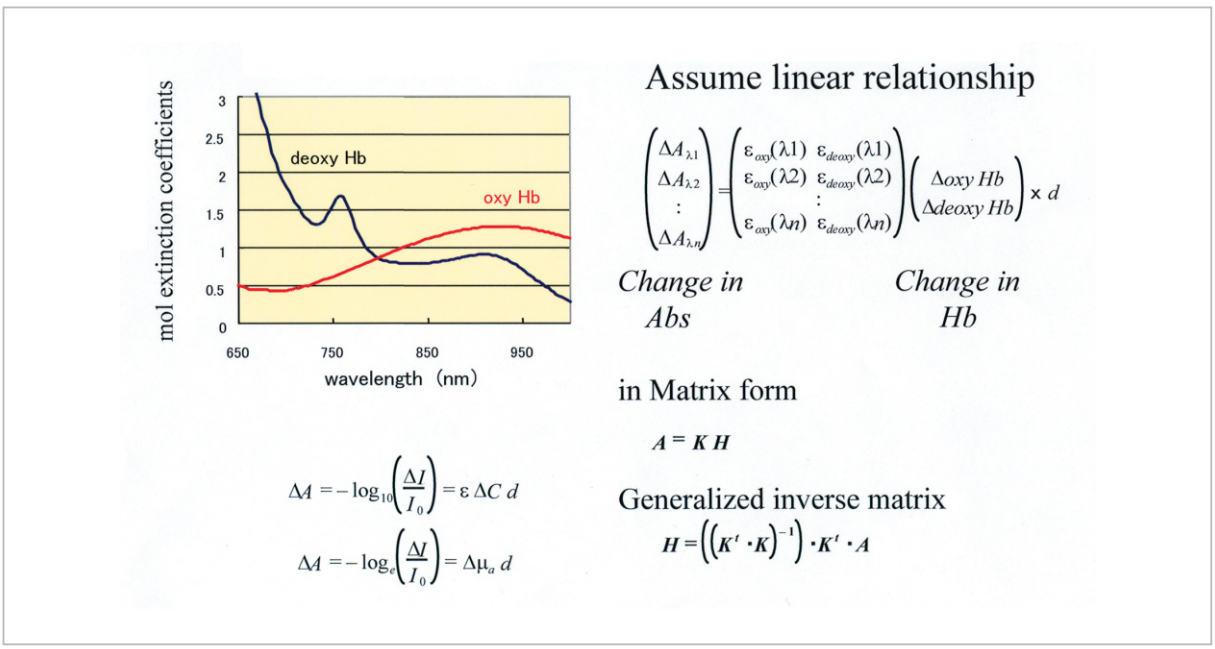

$$\Delta A = -\log_{10}\left(\frac{\Delta I}{I_0}\right) = \varepsilon\,\Delta C\,d$$

$$\Delta A = -\log_{e}\left(\frac{\Delta I}{I_0}\right) = \Delta\mu_a\,d$$

$$\begin{pmatrix}\Delta A_{\lambda 1}\\ \Delta A_{\lambda 2}\\ \vdots\\ \Delta A_{\lambda n}\end{pmatrix} = \begin{pmatrix}\varepsilon_{oxy}(\lambda 1) & \varepsilon_{deoxy}(\lambda 1)\\ \varepsilon_{oxy}(\lambda 2) & \varepsilon_{deoxy}(\lambda 2)\\ \vdots & \\ \varepsilon_{oxy}(\lambda n) & \varepsilon_{deoxy}(\lambda n)\end{pmatrix}\begin{pmatrix}\Delta oxy\,Hb\\ \Delta deoxy\,Hb\end{pmatrix} \times d$$

$$H = \left(\left(K^t \cdot K\right)^{-1}\right) \cdot K^t \cdot A$$

Fig.9 *Hb parameters calculation*

$$\phi(r) = \frac{1}{4\pi D}\frac{\exp\left(-\sqrt{\frac{\mu_a}{D}}\,r\right)}{r} = \frac{1}{4\pi D}\frac{\exp\left(-\mu_{eff}\,r\right)}{r}$$

$$\Delta A = \varepsilon \Delta C \langle d \rangle + \Delta S$$

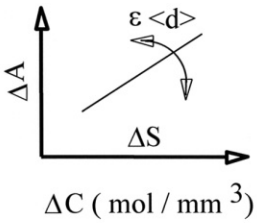

ΔC (mol / mm ^{3})

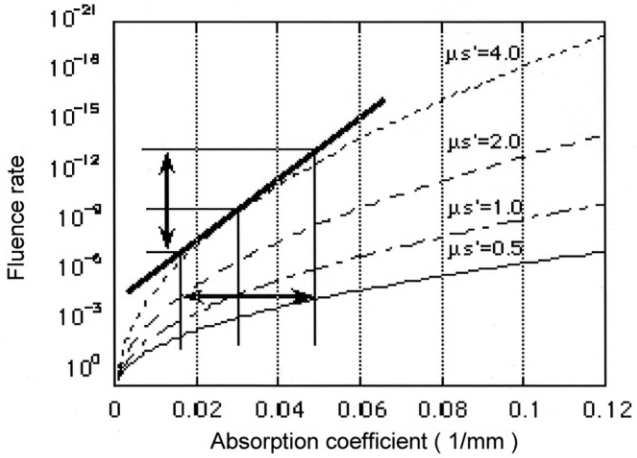

Fig.10 *Analytical solution of the Diffusion equation*

the position of contact. Without a change in absorbance, no change in concentration will occur as far as the modified Lambert-Beer's law is concerned. In other words, the measurement start time that provides the point of reference is always zero. This means that care must be taken when comparing measured data between different subjects or data measured at different times.

5 Brain activity measurement by near infrared light

The near infrared light used for somatometry is of wavelengths in the vicinity of 800 nm. Light in this wavelength region easily penetrates the living body for two reasons: it is subject to particularly low absorption in water (at wavelengths longer than 1,000 nm, light is sharply absorbed by water) and to low absorption in the blood (at wavelengths shorter than 600 nm, light is sharply absorbed by hemoglobin in the blood). Therefore, these wavelengths can be used to acquire information on the interior of the living body in the same fashion as X-rays. Figure 11 shows an optical absorption spectrum of water at wavelengths from 200 nm to 100,000 nm [14]. From the figure, it can be seen that absorption is low in the vicinity of 800 nm.

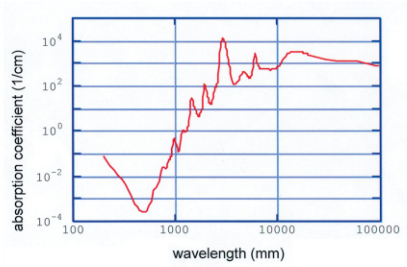

G. M. Hale and M. R. Querry, "Optical constants of water in the 200 nm to 200 μm wavelength region," Appl. Opt., 12, 555--563, (1973).

Fig.11 *Water spectra*

Research into somatometry systems using near infrared light was initiated with a report [15] by Jobsis published in 1977. This research began with the development of a single-channel oxygenation monitor [16] and application of this device [17], progressed to optical CT [18], and is now focused on optical topography [19] and near-infrared spectroscop-

ic (NIRS) imaging systems [20]. These systems calculate changes in oxyHb and deoxyHb as indexes of oxygen of the living body and display the Hb parameters together with the totalHb change, represented as the sum of these changes. It may be said that it was the development of optical topography that began to attract attention to brain-function research. Since these systems have spread so rapidly in brain research, it may be said that the accumulated background research described above in this article cannot have been subject to appropriate follow-up verification. While a generation of new researchers are beginning to familiarize themselves with near infrared imaging equipment, it seems to us that a growing chorus of dissenting voices are indicating the disadvantages of using this equipment in brain research. Optical measurement does offer several advantages relative to other brain-activity measurement instruments. However, we must avoid foregoing reliability simply for the sake of these advantages.

Here we will compare near-infrared and X-ray measurement. Since X-rays are absorbed strongly by bones, these appear as shadows in X-ray images. Moreover, since X-rays travel in nearly a straight line through the living body, bones will appear in images without blurring, as when an X-ray image is taken of the palm. X-rays are also absorbed by blood and tissues, in addition to bones. Since the relevant absorption coefficients are all known, if the scale of the displayed image is adjusted, a given target can be observed within the living body. Thus, since differences in the absorption coefficient correspond to tissue differences in the case of X-rays, visualization (i.e., imaging) of the living body becomes possible. On the other hand, when near infrared light is irradiated to the palm (inner side) and the palm is viewed from the outside with a dedicated camera, vessels, as opposed to bones, may be seen. This is because in the living body, near infrared light is strongly absorbed by the hemoglobin contained in the red blood cells in the blood, enabling an image of the vessel to be formed. (However, since these rays are simultaneously scattered by the tissues, the image suffers a certain degree of blurring.) At the same time, since the hemoglobin contained in the blood serves as an oxygen-transporting material, and changes color depending on its state of oxidation, the oxygenated state of hemoglobin can be calculated from the absorption coefficient measured with light at multiple wavelengths. In brief, unlike the structural image obtained using an X-ray, the use of multiple-wavelength near infrared light enables us to obtain a functional image of oxidation states.

6 Equipment for imaging optical absorption

Figure 12 shows the equipment we have manufactured for imaging light absorption, showing probes attached to the head of the subject. This consists of a light source (consisting of near-infrared semiconductor lasers at three wavelengths: 780 nm, 805 nm, and 830 nm), light guides (compound glass fibers), photodetectors (photomultiplier tubes), a control unit, a display unit, as well as additional components. This prototype device includes six sets of light-source and irradiation light guides, photodetectors, and photodetector light guides, enabling measurement of irradiation and reception using six device pairs. At present these can be extended to up to 16 sets. The device was designed to enable external analog input. The 12 strands of optical fiber (six strands for irradiation and six strands for light reception) are arranged in a predeter-

NIR OPTIM_A
Near infrared Optical imaging system

Fig. 12 *Optical systems*

mined manner and used in measurement, enabling image display. In order to perform this imaging, however, it is in principle first necessary to solve an inverse problem of light propagation. However, to avoid this initial step, variation of the optical signal is assumed to result only from hemoglobin change; signal values are then arranged and subjected to interpolation to form an image.

7 Measurement of occipital area during experimental visual stimulation

During visual stimulation using a checkerboard pattern, data is measured with the ends of optical fibers disposed on the scalp over the occipital area of the subject, as shown in Fig. 13. The optical measurement data is converted to an image of hemoglobin change and displayed superimposed on an MRI image to create the image shown in Fig. 14. An MRI image processed as an X-ray image was used as a template. This display enables us to measure hemodynamic response variation in the visual area for a given stimulus.

Figure 15 is an illustration of a process of signal analysis. The upper-right figure shows the timing of the stimulus. In this case, the task is given three times. The second figure in the right-hand column shows the measured data as absorbance (Abs) after logarithmic transformation, which serves as raw data for this process. Absorbance was subjected to baseline correction. Here, "baseline" refers to a straight line connecting the respective Abs values corresponding to the start of each task. The change in absorbance can be calculated by subtracting this baseline signal from the raw data. As can be understood from the upper right figure, it was determined that the light was able to capture a state of brain activity even without the addition of other data items. The change in the Hb parameter was calculated based on this change in absorbance to obtain the second figure in the right-hand column. The three data items are then added to obtain the figure at bottom right. From the

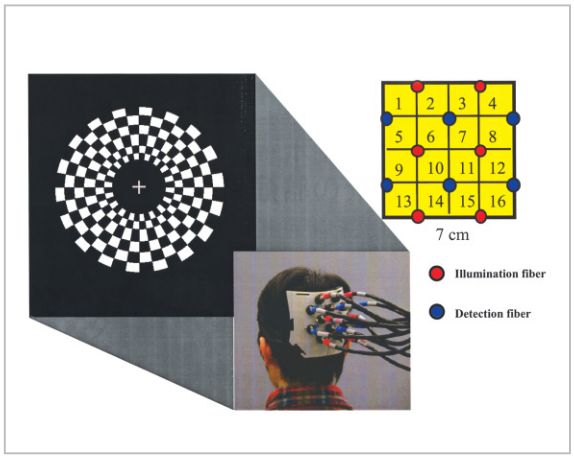

Fig. 13 Checkerboard

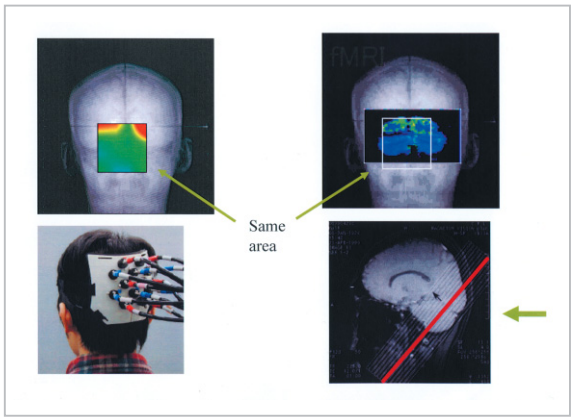

Fig. 14 NIRS image and fMRI

figure, it was found that oxyHb increases and deoxyHb decreases with a visual stimulus. These peak values are arranged, interpolated, and subsequently placed within an image to create the image shown in Fig. 14. In this experiment, temporal resolution was set to 0.5 seconds. In short, a single image can be displayed every 0.5 seconds; this means that the device is capable of capturing the dynamic activity of the brain with sufficient accuracy.

The data obtained is initially no better than a tile or check array, where the diagonals of each tile are formed by illumination and detection fibers because the two types of optical fibers are arranged alternately. A simple method of obtaining a topographic image involves two-dimensional interpolation of two or more items of initial data. Various mathematical interpolation procedures are available, such as linear interpolation and spline interpolation, and each procedure gives a slightly dif-

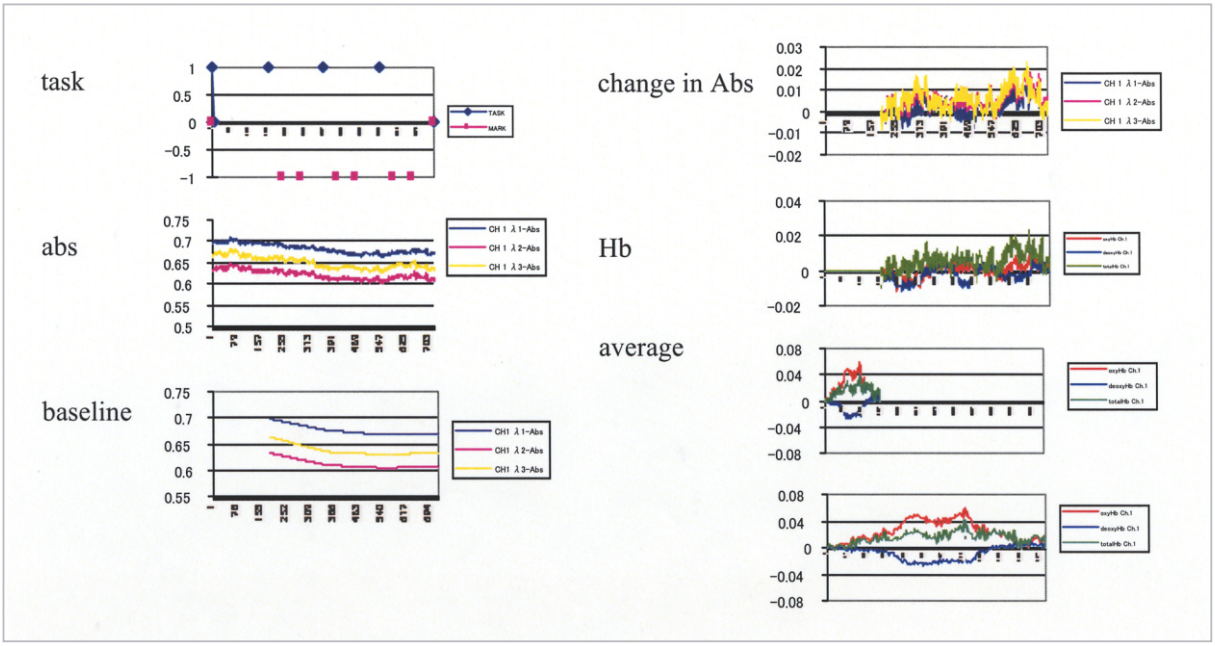

Fig. 15 *Signal analysis*

ferent image. Though interpolation among tile data is likely to improve the spatial resolution of images, we must keep in mind that the original data is in the form of tiles, not complete images. Discussion of the resolution of topography is hardly meaningful; if we consider the matter carefully, we must recognize that resolution merely consists of differences between interpolation procedures. Interpolation itself is an operation in which data is converted into an easy-to-view format, and cannot be viewed as a method of improving spatial resolution.

If spatial resolution is defined as the distance at which two elements can be distinguished one-dimensionally, the spatial resolution of a topographic image will, strictly speaking, be determined as three tiles, where the diagonals of each are formed by illumination and detection fibers. This is because empty spaces between image spaces must also be measured. Assuming that each tile side is 2.5 cm, three tiles will measure 7.5 cm.

In measuring the brain, it is safest to devise a task such that two or more activation sites are not located in an area as large as three tiles. In this experiment, the right and left brain areas corresponding to visual processes were successfully imaged.

8 Features of optical measurement equipment using near infrared light

As described above, a device displaying a topographic image using light is capable of displaying the extent of change in oxyHb, deoxyHb, and totalHb as an image in near real time with spatial resolution of a few centimeters and temporal resolution of 1 second or less.

The following can be proposed as advantages of optical measurement equipment:

- Ease of measurement
- Enables measurement near the subject
- Extremely low device maintenance and running costs, comparable to costs of EEG equipment
- High temporal resolution; capable of displaying Hb images at a rate of one or more frames per second in real time
- Excellent S/N ratio, thus images can be obtained without being subjected to statistical operation
- Subject may move slightly insofar as fibers are affixed to the head
- The equipment enables observation of hemodynamic response changes based on optical-absorption changes in hemoglobin

On the other hand, the following disadvantages may also be indicated:

- Concentration of hemoglobin not linearly related to hemoglobin amount as determined by light-based measurement
- In applying the diffusion equation, optical properties (absorption coefficient, scattering coefficient, phase function) of the human subject have yet to be determined
- Limited spatial resolution
- Difficult to resolve space among tissues in the direction of depth
- Despite ease of measurement, successful measurement is questionable, entailing verification of numerous factors, e.g., S/N ratio

The first drawback mentioned above represents a fundamental problem. As shown in Fig. 15, when the hemoglobin parameters are calculated based on absorbance, a generalized inverse matrix of Hb absorption spectrum values is used as the coefficients. The procedure is originally predicated on the linear relationship between the change in hemoglobin concentration and the change in the measured value. However, the solution of the diffusion equation reveals that this relationship is not linear. In other words, the gradient of the coefficient obtained by linear approximation between the hemoglobin concentration and the measured value varies depending on the initial values of the reduced scattering coefficient and the absorption coefficient (assumed as reference values in calculating the absorbance change). This gradient corresponds to what is known as the "optical path length factor." The value of this gradient must be verified to determine whether it remains the same from the initial time of measurement through the remainder of measurement. Various structures such as the cranial bone determine scattering and absorption patterns in the human head, which indicates that the functional image showing hemoglobin change is affected by the structural image of the head, as shown in Fig. 16.

9 Conclusion — What type of brain research makes most effective use of optical measurement? —

The advantages and disadvantages of optical measurement by near infrared light were described above. Essentially two points must be examined when applying this type of measurement to brain research. These points are

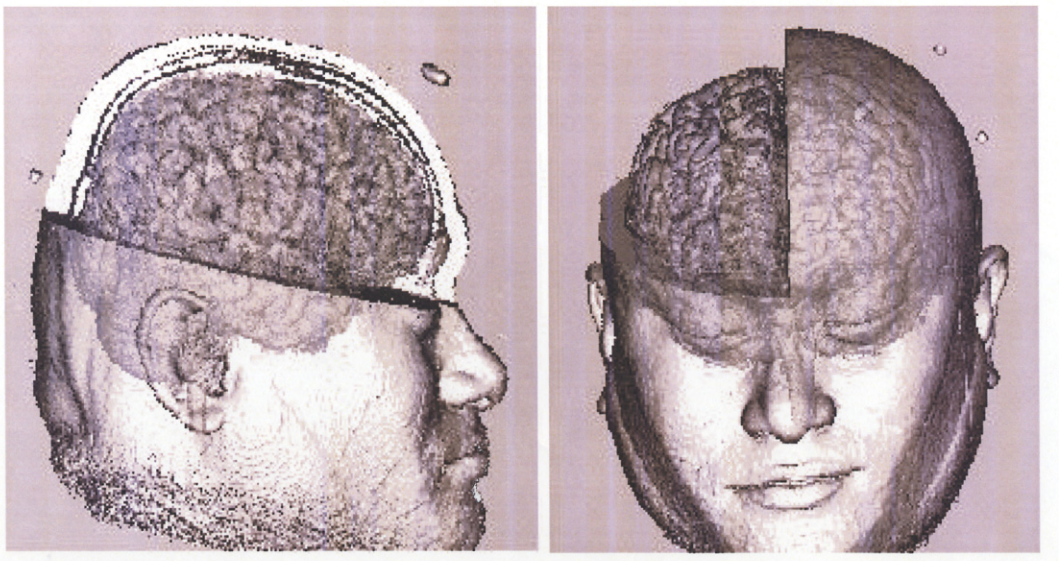

Fig. 16 *Structural image*

described below.

- If hemodynamic response information is to be obtained, fMRI is also available. However, quantitative values of oxyHb, deoxyHb, and totalHb cannot be measured by fMRI; whether these values are essential in the brain research in question should be considered.
- If mapping is the main purpose of the brain research, it is important to determine whether optical equipment featuring a certain spatial resolution can be used in practice.

The first point above involves differentiation from fMRI and the second point involves a question about the original goal of the brain research to be conducted by the researchers involved. Certainly, if optical measurement is used only to obtain data available using fMRI, optical measurement is not necessary. On the other hand, if the final purpose of the brain research is to search sites within the brain—i.e., mapping—equipment offering high spatial resolution must be employed.

However, there are cases in which fMRI measurement cannot be applied, as with measurement of infants. With optical measurement, an infant's brain can be measured while the child is held by the mother. Moreover, we have succeeded in measuring brain activity while the subject was exercising [21] [22]. This is data that cannot be provided by fMRI, EEG, or MEG devices. It is assumed that optical measurement can reveal brain activities accompanying actions, indicating potential applications in neuro-rehabilitation. We expect that future development will lead in this direction. Furthermore, in an increasing number of studies the interpretation of fMRI data is elucidated with the help of optical data [23]; we thus anticipate that optical measurement will develop into an essential component of brain research.

References

1 S. Ogawa, D. W. Tank, R. Menon, J. M. Ellermann, S. Kim, H. Merkle, and K. Ugurbil, "Intrinsic Signal Changes Accompanying Sensory Stimulation: Functional Brain Mapping with Magnetic Resonance Imaging", PNAS 89: 5951-5955, 1992.

2 S. F. Johnston, "A History of Light and Colour Measurement: Science in the Shadows", Institute of Physics Publishing, 2001.

3 F. J. Janssen, "A study of the absorption and scattering factors of light in whole blood", Med. & Biol. Engng. Vol.10, pp231-240, 1972.

4 A. Ishimaru, "Wave Propagation and Scattering in Random Media", Academic Press, 1978.

5 M. Born and E. Wolf, "Principes of Optics -Seventh edition", Cambridge University Press, 1999.

6 K. M. Case and P. F. Zweifel, "Linear Transport Theory,Addison-Wesley", 1967.

7 J. J. Duderstadt and L. J. Hamilton, "Nuclear Reactor Analysis", JOHN WILEY & SONS, 1942.

8 S. Chandrasekhar, "Radiative transfer", Dover, 1960.

9 J. M. Kaltenbach and M. Kashke, "Frequency- and Time-domain modeling of light transport in random media", Medical Optical Tomography, SPIE IS 11, 65-86, 1993.

10 K. Furutsu and Y. Yamada, "Diffusion approximation for a dissipative random medium and the applications", Phys. Rev. E, 50, 3634-3640,1990.

11 D. T. Delpy, M. Cope, P. van der Zee, S. Arridge, S. Wray, and J. Wyatt, "Estimation of optical pathlength through tissue from direct time of flight measurement", Phys. Med. Biol. 33, 1433-1442, 1988.

12 S. J. Matcher, C. E. Elwell, C. E. Cooper, M. Cope, and D. T. Delpy, "Performance comparison of several published tissue near-infrared spectroscopy algorithms", Analytical Biochemistry, 226, 54-68, 1995.

13 W. G. Zijlstra, A. Buursma, and W. P. Meeuwsen-van der Roest, "Absorption spectra of human fetal and

adult oxyhemoglobin, de-oxyhemoglobin, carboxyhemoglobin, and methemoglobin", Clin. Chem. 37, 1633-1638, 1991.

14 G. M. Hale and M. R. Querry, "Optical constants of water in the 200 nm to 200μm wavelength region", Appl. Opt., 12, 555--563, 1973.

15 F. F. Jobsis, "Noninvasive, Infrared Monitoring of Cerebral and Myocardial Oxygen Sufficiency and Circulatory Parameters", Science, 198, 1264-1267, 1977.

16 T. Tamura, H. Eda, M. Takada, and T. Kubodera, "New instrument for monitoring hemoglobin oxygenation", Adv Exp Med Biol, 248 : 103-107, 1989.

17 H. Eda, I. Oda, Y. Ito, Y. Wada, Y. Oikawa, Y. Tsunazawa, M. Takada, Y. Tsuchiya, Y. Yamashita, M. Oda, A. Sassaroli, Y. Yamada, and M. Tamura, "Multichannel time-resolved optical tomographic imaging system", Review of Scientific Instruments, Sep/1999, Vol.70, Issue.9, pp.3595-3602,1999.

18 S. Homma, H. Eda, S. Ogasawara, and A. Kagaya, "Near-infrared estimation of O2 supply and consumption in forearm muscles working at varying intensity", J. Appl. Physiol., 80(4),pp1279-1284,1996.

19 A. Maki, Y. Yamashita, Y. Ito, E. Watanabe, Y. Mayanagi, and H. Koizumi, "Spatial and temporal analysis of human motor activity using noninvasive NIR topography", Med Phys. 22(12), 1997-2005, 1995.

20 H. Eda, I. Sase, A. Seiyama, H. C. Tanabe, T. Imaruoka,Y. Tsunazawa, and T. Yanagida, "Optical Topography System for Functional Brain Imaging:Mapping human occipital cortex during visual stimulation", Proceedings of Inter-Institute Workshop on In Vivo Optical Imaging at the NIH, OSA, 93-99, 2000.

21 I. Miyai, H. C. Tanabe, I. Sase, H. Eda, I. Oda, I. Konishi, Y. Tsunazawa, T. Suzuki, T. Yanagida, and K. Kubota, "Cortical Mapping of Gait in Humans: A Near-Infrared Spectroscopic Topography Study, NeuroImage", Volume 14, Issue 5, 1186-1192, 2001.

22 H Eda, I Miyai, K Kubota, and T Yanagida, "Cortical mapping of gait by Near infrared spectroscopic imaging Rinsyo Noha", Vol.44, No.12, 751-757,2002.(in Japanese)

23 H Eda, I Sase, A Takatsuki, A Seiyama, T Yanagida, and S Miyauchi, "BOLD Signal by fMRI agrees eith totalHb signal by NIR imaging system", Technical report of IEICE.MBE2001-97,95-99,2001. (in Japanese)

EDA Hideo, *Ph.D.*

Expert Researcher, Brain Information Group, Kansai Advanced Research Center, Basic and Advanced Research Department

Biomedical Engineering, Medical Optics